HHS Public Access

Author manuscript

Ann Thorac Surg. Author manuscript; available in PMC 2015 July 30.

Published in final edited form as:

Ann Thorac Surg. 2011 September ; 92(3): 797–803. doi:10.1016/j.athoracsur.2011.04.047.

Saddle-Shape Annuloplasty Increases Mitral Leaflet Coaptation after Repair for Flail Posterior Leaflet

Mathieu Vergnat, MD[5], **Benjamin M. Jackson, MD**[1,5], **Albert T. Cheung, MD**[2], **Stuart J. Weiss, MD, PhD**[2], **Sarah J. Ratcliffe**[4], **Mathew J. Gillespie, MD**[3,5], **Y. Joseph Woo, MD**[1], **Joseph E. Bavaria, MD**[1], **Michael A. Acker, MD**[1], **Robert C. Gorman, MD**[1,5], and **Joseph H. Gorman III, MD**[1,5]

[1]Department of Surgery, University of Pennsylvania, Philadelphia

[2]Department of Anesthesia, University of Pennsylvania, Philadelphia

[3]Department of Pediatrics, University of Pennsylvania, Philadelphia

[4]Department of biostatistics & Epidemiology, University of Pennsylvania, Philadelphia

[5]Gorman Cardiovascular Research Group, University of Pennsylvania, Philadelphia

Abstract

Background—The primary goal of mitral repair surgery is the re-establishment of normal leaflet coaptation. Surgical techniques which maintain or restore leaflet geometry promote leaflet coaptation. Recent three-dimensional (3D) echocardiographic studies have shown that saddle-shape annuloplasty has a salutary influence on leaflet geometry. Therefore, we hypothesized saddle-shaped annuloplasty would improve leaflet coaptation in repair cases for flail posterior leaflet segments.

Methods—Sixteen patients with a flail posterior segment and severe MR had valve repair using standard techniques. Eight patients received a saddle-shaped annuloplasty and eight received flat annuloplasty. Real-time 3D transesophageal echocardiography was performed before and after repair. Images were analyzed using a custom software to calculate mitral annular area (MAA), septolateral dimension (SL), Intercommissural width (CW), total leaflet area (TLA) and leaflet coaptation area (LCA).

Results—Post-repair mitral annular area (flat − 588.6 ± 26.5 mm^2; saddle − 628.0 ± 35.3 mm^2, p= 0.12) and total leaflet area (flat − 2198.5 ± 151.6 mm^2; saddle − 2303.9 ± 183.8 mm^2, p= 0.67) were similar in both groups. Post-repair leaflet coaptation area was significantly greater in the saddle group than in the flat group (226.8 ± 24.0 mm^2 and 154.0 ± 13.0 mm^2, respectively, p= 0.02).

Address Correspondence to: Joseph H. Gorman, III, MD, Gorman Cardiovascular Research Group, Glenolden Research Laboratory, University of Pennsylvania, 500 S. Ridgeway Avenue, Glenolden, PA 19036, Phone: 267-350-9616, FAX: 267-350-9627, gormanj@uphs.upenn.edu.

Conclusion—Real-time 3D echocardiography and novel imaging software provides a powerful tool for analyzing mitral leaflet coaptation. When compared to flat annuloplasty saddle-shaped annuloplasty improves leaflet coaptation area after mitral valve repair for severe mitral regurgitation secondary to a flail posterior leaflet segment. Use of saddle-shaped annuloplasty devices may increase repair durability. (245 Words)

Keywords

Echocardiography; Imaging; Mitral Regurgitation; Mitral Valve Repair

Introduction

Since its inception forty years ago mitral valve repair surgery has become progressively more intricate. [1] Despite this growing complexity there is still consensus that three basic tenets remain fundamental to a successful repair: remodeling annuloplasty, preservation of mobile leaflet tissue, and restoration of a large surface of leaflet coaptation. [2,3] Some authors propose that the creation of a large area of leaflet coaptation is the primary goal of the repair surgeon with annuloplasty and leaflet preservation serving as important tools toward that end. [4]

Though many techniques have been developed to spare and mobilize leaflet tissue little recent attention has been paid to the influence of annuloplasty on leaflet coaptation. [4,5,6] Relying on surgical intuition and careful but qualitative observation Carpentier proposed early on that ring annuloplasty optimizes coaptation by restoring more normal annular size and shape. [2,7] While this intuitive assertion is widely accepted little quantitative evidence exists.

The development of quantitative three-dimensional (3D) echocardiographic imaging techniques has expanded our understanding of normal mitral annular geometry. [8,9] These insights have spawned a new generation of saddle-shaped annuloplasty rings designed to restore the annulus to its normal 3D geometry. We have shown previously that saddle-shaped annuloplasty restores or maintains normal annular geometry and in doing so reestablishes more normal leaflet geometry [10] and function [11] when compared to flat annuloplasty. Based on this work and Carpentier's premise, we hypothesized that saddle-shaped annuloplasty promotes a larger area of leaflet coaptation after mitral valve repair. To test this hypothesis we applied real-time 3D echocardiography (rt-3DE) and novel image analysis software to a cohort of patients undergoing mitral valve repair for mitral regurgitation secondary to a flail segment of the posterior leaflet.

Patients and Methods

Patients

Sixteen patients with severe mitral regurgitation secondary to a flail segment of the posterior leaflet (15 P2, 1 P3) underwent mitral valve repair by four surgeons. The flail segment was treated by triangular resection, quadrangular resection, or leaflet inversionplasty (see Table 1 for a summary of repair techniques).

In all cases ring selection was at the discretion of the surgeon and the study was done retrospectively. In 8 patients a Carpentier-Edwards Phyiso Annuloplasty Ring (flat ring; Edwards Lifesciences, Irvine, CA) was used. In the other 8 patients a Medtronic Profile 3D™ Annuloplasty System (saddle ring, Medtronic, Minneapolis, MN) was placed.

The inversionplasties were carried out by grasping the leading edge of the ruptured chordal segment with forceps and inverting it into the left ventricle. This technique moves a triangular piece of posterior leaflet tissue below the plane of the mitral valve annulus and presents two opposing short lines of tissue along the residual P2 segment. These two lines were then re-approximated with the double running suture. Static pressure testing of the ventricle at this point uniformly demonstrated a competent mitral valve. The repair was then reinforced with ring annuloplasty, paying attention to size the ring appropriately to the entire pressurized mitral valve orifice. [12]

The triangular and quadrangular resections where carried out using standard Carpentier techniques. [13] For each technique a minimum of leaflet tissue was resected and the remaining leaflet edges approximated and sutured. In all cases of quadrangular resection the annulus was plicated. Repairs where then reinforced with annuloplasty rings which were sized to the anterior leaflet.

All patients underwent rt-3DE for mitral valve imaging before and after repair. The before repair imaging was performed in the operating room after induction of general anesthesia and before sternotomy. Post repair images were obtain after sternal closure prior to leaving the operating room.

The rt-3DE data sets were acquired, through mid-esophageal view, with an iE-33 platform (Philips Medical Systems, Andover, MA) equipped with a 2- to 7-MHz X7-2t TEE matrix transducer. Electrocardiographically gated full-volume images were acquired over 4 cardiac cycles during a period of apnea at end expiration. Care was taken to include the mitral apparatus in its entirety for the volumetric data during the entire acquisition. The volumetric frame rate was 17 to 30 frames/s with an imaging depth of 12 to 16 cm.

The study protocol was reviewed and approved by the University of Pennsylvania School of Medicine Institutional Review Board.

Image Segmentation

Each full-volume data set was then exported to an Echo-View 5.4 (Tomtec Imaging Systems, Munich, Germany) workstation for image analysis. Analysis was performed at mid-systole and mid-diastole. The plane of the mitral valve orifice was rotated into a short-axis view. The geometric center was then translated to the intersection of the two corresponding long-axis planes which then corresponded to the intercommissural and septolateral axes of the mitral valve orifice. A rotational template consisting of 18 long-axis cross-sectional planes separated by 10 degree increments was superimposed on the 3-dimensional echocardiogram. The two annular points intersecting each of the 18 long-axis rotational planes were then identified by means of orthogonal visualization of each plane; the two annular points were marked interactively (Figure 1).

Measurement planes were then marked at fixed 1-mm intervals along the entire length of the intercommissural axis (Figure 2A). In each two-dimensional (2D) plane, data points delineating anterior and posterior leaflets were traced across the atrial surfaces resulting in a 500- to 1000-point data set for each valve (Figure 2B). For the coaptation tracing, meticulous care was taken to clearly identify the tip of both anterior and posterior leaflets immediately before coaptation (using previous frames), so that the highest (most atrial) and lowest (most ventricular) margins of the coaptation zone could be defined. These atrial and ventricular edges of the coaptation zone were then marked interactively (Figure 2B, C). Anterior and posterior commissures (AC, PC) were defined as annular points at the junction between the anterior and posterior leaflets (middle of commissural region) and interactively identified. The X, Y, Z coordinates of each data point, assigned to the annulus, anterior leaflet, posterior leaflet, or the coaptation surface were then exported to Matlab (The Mathworks, Inc, Natick, Mass).

To assess total leaflet tissue the anterior and posterior leaflet were imaged again at end diastole using the same techniques.

Annular Analysis

Using custom Matlab algorithms (Mathworks Inc., Natick, MA, USA) and orthogonal distance regression, the least squares plane of the data point cloud for the annulus was aligned to the x-y plane. Under these geometric conditions, the annular height for each point (z_n) was plotted as a function of rotational position on the annulus. A number of anatomic landmarks (Figure 3) were identified. The septum (S) was identified as the anterior horn of the annulus at the aortic valve, corresponding to z_{max}. The lateral annulus (L) was located at the middle of the posterior annulus circumference. With the annular model transformed such that the commissures were aligned with the y-axis, the anterolateral (AL) and posteromedial (PM) annular points are the locations of maximal and minimal y-value.

Annular height (AH) was defined as $z_{max} - z_{min}$. Septolateral (SL) diameter was defined as the distance, in 3D space, separating the two data points S and L. Commissural Width (CW) was defined as the 3D distance between the two commissures. Annular height to commissural width ratio (AHCWR) was subsequently defined as AH/CW × 100%. Mitral annular area (MAA) was defined as the area enclosed by the 2D projection of a given annular data set onto its least squares plane.

The degree of annular under-sizing post repair was calculated as the change in annular area (post MAA – pre MAA) divided by pre repair MAA and expressed as a percentage.

Coaptation and Leaflet Analysis

Using interpolation methods, the 3D length of atrial and ventricular coaptation edges were determined. The 3D coaptation area and diastolic total leaflet area (TLA) were then determined by triangulating the sampling points and summing the areas of the individual triangles.

Since leaflet coaptation area is known to be directly proportional to total leaflet area and inversely proportional to annular size a normalized coaptation area (NCA) was calculated to

reduce between patient variation in these post-repair parameters and to more clearly isolate the influence of annuloplasty shape on coaptation area:

NCA = leaflet coaptation area *(MAA / TLA)

To provide a 2D visual representation of the coaptation area the atrial and ventricular coaptation edges were projected on to a viewing plane orthogonal to the least squares annular plane passing through both commissures (Figure 2C). Averaged images were then created for each group using interpolation of a normalized intercommissural sampling scale. The resulting images were then centered for comparison.

From these 2D projections the leaflet coaptation length was calculated at every point from commissure to commissure and plotted for each group using normalized intercommissural distances.

All image analysis was done retrospectively.

Statistical Analyses

All continuous annular and leaflet parameters for the two groups (Table 1) were compared using either Kruskal-Wallis rank sum test or t-test, depending on normality assumptions being met. The central tendency of these measurements is presented as mean ± standard error of the mean.

Because of the non-continuous nature of the annuloplasty ring data between group comparisons were carried out using Mann-Whitney u-tests and the central tendency is reported as the median.

Overall assessment of leaflet coaptation length and overall coaptation area shape between groups were carried out using a mixed effects model to account for the correlation between positions inherent in the two groups. Subsequently, coaptation length was compared at each position along the intercommissural line using a Wilcoxon exact test without correction for multiple comparisons.

For all comparisons, $p \leq 0.05$ was considered significant. All statistical analyses were performed using Stata 11.0 MP (StataCorp LP, College Station, TX).

Results

Annulus

The median nominal annuloplasty ring size was 32 in each group and the full range of ring sizes is presented in Table 1.

Measured and derived annular parameters are summarized in Table 2. All values are expressed as mean ± standard deviation. Data are presented for the flat ring (n=8) and saddle ring (n=8) groups before and after repair.

Prior to repair annular sizes, as assessed by MAA, SLD and CW, were similar in both groups. After repair both groups' annular dimensions were significantly but similarly

reduced. After flat annuloplasty MAA was diminished by 50.7 ±2.8% and by 54.5±4.9% after saddle annuloplasty (p=0.40). After repair all measures of annular size (MAA, SLD, CW) were similar in both groups.

Global annular height was maintained (pre − 7.5 ± 0.6mm; post − 7.7 ± 0.5mm) after saddle annuloplasty, and significantly reduced by flat annuloplasty (pre − 7.2 ± 0.9mm; post − 2.7 ± 0.2mm, p = 0.00). The non-planarity of the annulus, as assessed by the AHCWR, also showed a significant decrease after flat annuloplasty (pre − 20.2 ± 1.6%; post − 8.7 ± 0.6%, p = 0.00). AHCWR was maintained by saddle-shape annuloplasty (pre − 20.4 ± 1.6%; post 22.9 ± 1.2%).

Leaflets

Total post repair leaflet surface area was similar between groups (flat − 2198.5 ± 151.6 mm^2 vs. saddle − 2303.9 ± 183.8 mm^2). The 3D coaptation area was found to be significantly larger in the saddle annuloplasty group (flat − 154.0 ± 13.0 mm^2 vs. saddle − 226.8 ± 24.0mm^2 p = 0.02). The fraction of total leaflet area involved in the coaptation region was also greater in the saddle group (flat − 0.07 ± 0.00 vs. saddle − 0.10 ± 0.01 p = 0.00).

Even though there were no significant between group differences in MAA and TLA the NCA illustrated the most dramatic between group differences with the saddle group NCA being more than 50% larger than the flat repair group (62.6 ± 7.7 mm2 vs. 42.2 ± 2.7 mm^2 p = 0.01).

Additionally, both the atrial and the ventricular 3D coaptation lines were found to be longer in the saddle group (see Table 2).

Figure 4 demonstrates a 2D projection of the averaged leaflet coaptation areas for each group. From this figure it can be seen that the coaptation area and length of the atrial and ventricular coaptation edges of the flat group are remarkably smaller than the saddle group. The relationship of the coaptation lines and commissures to the annular plane is also illustrated. In the flat ring group commissure and coaptation lines are pulled closer to the annular plane.

A comparison of leaflet coaptation lengths as a function of normalized intercommissural position is shown in Figure 5. Considering all coaptation length measurements together the saddle group had, on average, coaptation lengths that were 1.44 times as long as the flat group (p=0.031). The regions where the coaptation lengths were found be significantly longer in the saddle group are shown by the shaded regions in Figure 5. The shape of the coaptation area was found to be similar in both groups.

Comment

The primary component of a durable mitral valve repair is the restoration of an *optimal* area of leaflet coaptation. [2,4] The word optimal applies to both the size and shape of the coaptation region. The factors that influence coaptation are annular size, annular shape and the amount of mobile leaflet tissue. Surgeons can manipulate the first two factors via ring annuloplasty and the latter by growing number of surgical techniques.

The current study takes our understanding of the influence of annuloplasty on post repair leaflet coaptation literally to a new dimension. Prior to our previous work, re-establishment of *normal* annular geometry referred only to 2D relationships (i.e. - the normal systolic 4:3 ratio between the transverse and anteroposterior annular dimensions). [7] During the past decade, using a variety of imaging modalities we have been able to quantify the normal saddle shape [9,14,15] of the mitral valve and document its importance in optimizing valve performance. [11] These findings have lead to a new generation of saddle-shaped annuloplasty rings. Saddle-shaped rings have subsequently been shown to maintain more optimal patterns of leaflet geometry when compared to flat rings. [10,16,17] Based on these studies we hypothesized that saddle annuloplasty would have a strong beneficial effect on leaflet coaptation.

Using both previously developed 3D echocardiographic techniques [8, 9, 18] and the new algorithms described above we were able to demonstrate the positive influence of saddle annuloplasty on leaflet coaptation after repair for a flail posterior leaflet. Figure 4 is a powerful visual representation of the results. This figure illustrates the geometry, size, orientation and relationship to the annular plane of the coaptation areas of both groups. It can be seen that the flat ring elevates (“atrializes”) the leaflet commissures and in doing so shortens both the atrial and ventricular coaptation edges.

Figure 5 graphically compares leaflet coaptation height across the entire coaptation zone in both groups. This figure demonstrates regional heterogeneity in the difference in coaptation length between the two groups. The saddle ring most profoundly augments coaptation length in the region midway between the commissures and the center of the valve bilaterally. This figure highlights the strength of our 3D imaging methodology. The technique is not influenced by asymmetry of leaflet closure or asymmetry of coaptation along the mitral valve and, therefore, has the potential to overcome many of the limitations of 2D imaging. The standard evaluation of leaflet coaptation provided by 2D echocardiography is a one-dimensional coaptation length usually obtained as close to the valve center as possible. [19,20] Figure 5 demonstrates that the saddle-shaped ring influences coaptation length least in the middle of the valve. As a result 2D echocardiographic imaging directed at this region would have drastically under estimated the influence of ring shape on leaflet coaptation.

The primary goal of this study was to isolate the influence of annuloplasty ring shape on leaflet coaptation area. Because post repair total leaflet tissue and annular size also strongly contribute to leaflet coaptation, variations in operative technique and surgeon preference were strong possible confounding variables in this study. While differences in surgical technique to treat the flail leaflet segment (resection vs. inversionplasty) and ring size selection were not controlled for, the novel imaging techniques used provided documentation that both repair groups, were similar with regard to post repair TLA and MAA. To further control for the potential influence of these variables we normalized the coaptation area to both TLA and post repair MAA. Interestingly, this NCA parameter demonstrated an even more dramatic distinction between the two groups, lending further support to the conclusion that there was limited confounding influence due to between group variation in leaflet tissue or ring size.

Real-time 3D echocardiography is now available in both transthoracic and transesophageal modalities. The combination of this new technology and our novel image analysis algorithms provide the tools for quantifying the influence of repair techniques on the complex and dynamic geometry of the mitral valve. Our methodology is not influenced by viewing plane selection or annular distortions and, therefore, represents a potentially useful, clinically relevant, and consistent technique for quantitatively assessing mitral valve repair in vivo. With more clinical experience and longer term follow up it may ultimately be possible to correlate parameters such as NCA with repair durability.

Acknowledgments

This research project was supported by grants from the National Heart, Lung and Blood Institute of the National Institutes of Health, Bethesda, MD, (HL63954 and HL73021). It was also supported by an investigator initiated grant from Medtronic, Minneapolis, MN. R. Gorman and J. Gorman are supported by individual Established Investigator Awards from the American Heart Association, Dallas, TX. M. Vergnat was supported by a French Federation of Cardiology Research Grant.

Abbreviations and Acronyms

AH	Annular Height
AHCWR	Annular Height to Commissural Width Ratio
AA	Anterior Annulus
AC	Anterior Commissure
AML	Anterior Mitral Leaflet
AoV	Aortic Valve
CW	Commissural Width
LA	Left Atrium
LV	Left Ventricle
LVOT	Left Ventricular Outflow Tract
NCA	Normalized Coaptation Area
MAA	Mitral Annular Area
PA	Posterior Annulus
PC	Posterior Commissure
PML	Posterior Mitral Leaflet
SLD	Septolateral Dimension
TLA	Total Leaflet Area

References

1. Carpentier, A.; Adams, DH.; Filsoufi, F. Carpentier's Reconstructive Valve Surgery. Maryland Heights, MO: Saunders-Elsevier; 2010. p. V-VI.

2. Carpentier A. Cardiac valve surgery—the “French correction”. J Thorac Cardiovasc Surg. 1983; 86:323–337. [PubMed: 6887954]
3. Adams DH, Rosenhek R, Falk V. European Heart Journal. 2010; 31:1958–1967. [PubMed: 20624767]
4. Perier P, Hohenberger W, Lakew F, et al. Toward a New Paradigm for the Reconstruction of Posterior Leaflet Prolapse: Midterm Results of the “Respect Rather Than Resect”. Approach. Ann Thorac Surg. 2008; 86:718–725. [PubMed: 18721552]
5. Grossi EA, Galloway AC, Kallenbach K, et al. Early results of posterior leaflet folding plasty for mitral valve reconstruction. Ann Thorac Surg. 1998; 65:1057–1059. [PubMed: 9564927]
6. Mihaljevic T, Blackstone EH, Lytle BW. Folding valvuloplasty without leaflet resection: simplified method for mitral valve repair. Ann Thorac Surg. 2006; 82:e46–e48. [PubMed: 17126091]
7. Carpentier, A.; Adams, DH.; Filsoufi, F. Carpentier’s Reconstructive Valve Surgery. Maryland Heights, MO: Saunders-Elsevier; 2010. Techniques in Type 1 Dysfunction; p. 64
8. Jassar AS, Brinster CR, Vergnat V, et al. Quantitative Mitral Valve Modeling using Real-Time 3D-Echocardiography –Technique and Repeatability. Ann Thorac Surg. 2011; 91:165–171. [PubMed: 21172507]
9. Ryan LP, Jackson BM, Enomoto Y, Parish L, Plappert TJ, St. John-Sutton MB, Gorman RC, Gorman JH III. Description of Regional Mitral Annular Non-planarity in Healthy Human Subjects: A Novel Methodology. Journal of Thoracic and Cardiovascular Surgery. 2007; 134:644–648. [PubMed: 17723812]
10. Ryan LP, Jackson BM, Hamamoto H, et al. The Influence of Annuloplasty Ring Geometry on Mitral Leaflet Curvature. Ann Thorac Surg. 2008; 86:749–760. [PubMed: 18721556]
11. Salgo IS, Gorman JH III, Gorman RC, et al. Effect of Annular Shape on Leaflet Curvature in Reducing Mitral Leaflet Stress. Circulation. 2002; 106:711–717. [PubMed: 12163432]
12. Woo YJ. Minimally Invasive Valve Surgery. Surg Clin N Am. 2009; 899:923–949. [PubMed: 19782845]
13. Carpentier, A.; Adams, DH.; Filsoufi, F. Carpentier’s Reconstructive Valve Surgery. Maryland Heights, MO: Saunders-Elsevier; 2010. Techniques in Type II Posterior Leaflet Prolapse; p. 115-127.
14. Gorman JH III, Gupta KB, Streicher JS, et al. Dynamic Three-Dimentional Imaging of the Mitral Valve Using Rapid Sonomicrometry Array Localization. J Thorac Cardiov Sur. 1996; 112:712–725.
15. Gorman JH III, Jackson BM, Enomoto Y, Gorman RC. The Effect of Regional Ischemia on Mitral Valve Annular Saddle Shape. Ann Thorac Surg. 2004; 77:544–548. [PubMed: 14759435]
16. Mahmood F, Subramanian B, Gorman JH III, et al. Three-Dimensional Echocardiographic Assessment of Changes in Mitral Valve Geometry after Valve Repair. Ann Thorac Surg. 2009; 88:1838–1844. [PubMed: 19932245]
17. Mahmood F, Gorman JH III, Subramanian B, et al. Changes in Mitral Valve Annular Geometry After Repair Saddle Shaped vs. Flat Annuloplasty Rings. Ann Thorac Surg. 2010; 90:1212–1220. [PubMed: 20868816]
18. Ryan LP, Jackson BM, Eperjesi TJ, Plappert T, St. John Sutton M, Gorman RC, Gorman JH III. Regional Assessment of Human Mitral Leaflet Curvature Using Real-Time Three-Dimensional Echocardiography. Journal of Thoracic and Cardiovascular Surgery. 2008; 136:726–734. [PubMed: 18805278]
19. Yamauchi T, Taniguchi K, Kuki S, et al. Evaluation of the mitral valve leaflet morphology after mitral valve reconstruction with a concept “coaptation length index”. J Card Surg. 2005; 20:432–435. [PubMed: 16153273]
20. Gogoladze G, Dellis SL, Donnino R, et al. Analysis of the Mitral Coaptation Zone in Normal and Functional Regurgitant Valves. Ann Thorac Surg. 2010; 89:1158–1162. [PubMed: 20338324]

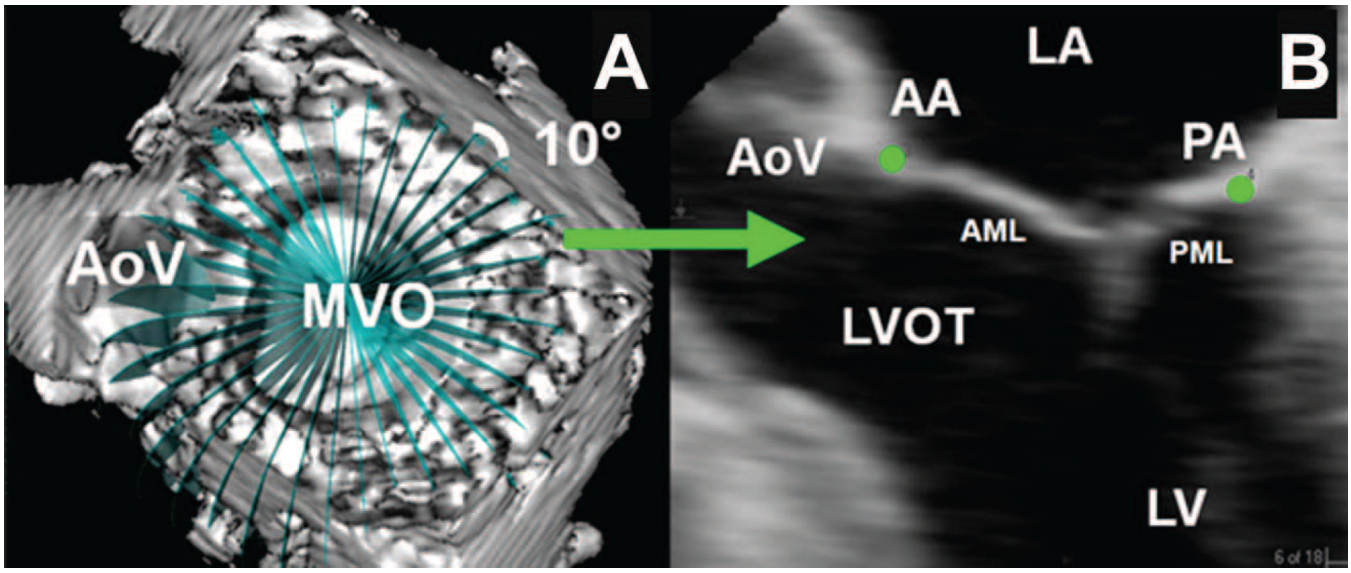

Figure 1. Annular Segmentation Technique

Panel A demonstrates a view of the mitral valve where the selected short axis plane coincides with the plane of the mitral valve. The aorta valve (AoV) and mitral valve orifice (MVO) are indicated. A rotational template consisting of 18 long axis planes evenly spaced at 10° increments and centered at the geometric center of the mitral valve are constructed. **Panel B** demonstrates a single long axis view (0 degrees on the rotational template of Panel A) of the heart. The left ventricle (LV), left ventricular outflow tract (LVOT), anterior (AML) and posterior (PML) mitral leaflets, left atrium (LA), aortic valve (AoV), anterior (AA) and posterior (PA) annular points have been marked. Note that in this orientation, the negative z-axis (for purposes or annular height and coaptation height calculations) extends towards the apex while the positive z-axis extends towards the left atrium.

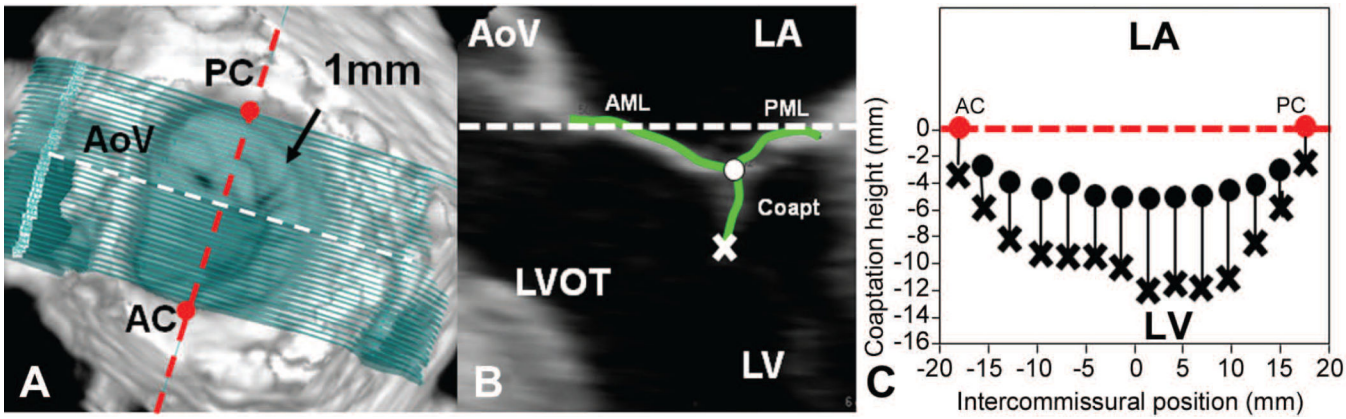

Figure 2. Leaflet Segmentation Technique

Panel A demonstrates leaflet segmentation using transverse cross-sections every 1 mm along intercommissural axis (anterior commissure – AC, posterior commissure – PC). **Panel B** demonstrates one of the 2D cross-sections represented by the white dashed line in panel A. In each of these septolateral measurement planes, between 5 and 40 individual points (depending on the septolateral diameter of the MV at the position of a given measurement plane) on the atrial surface of the MV are manually marked (green curves). The position of each point is recorded as anterior mitral leaflet (AML), coaptation leaflet (coapt) or posterior mitral leaflet (PML). The most atrial coaptation point is marked with an **O** while the most ventricular coaptation point is marked with an **X. Panel C** is a schematic which demonstrates how the atrial and ventricular coaptation points are then projected onto a viewing plane orthogonal to the least squares annular plane passing through the commissures to construct a 2D representation the atrial (**O**'s) and ventricular (**X**'s) coaptation edges. The area bounded by these coaptation lines is defines the coaptation area in this projection. The white and red dashed lines are both within least squares annular plane in all three panels.

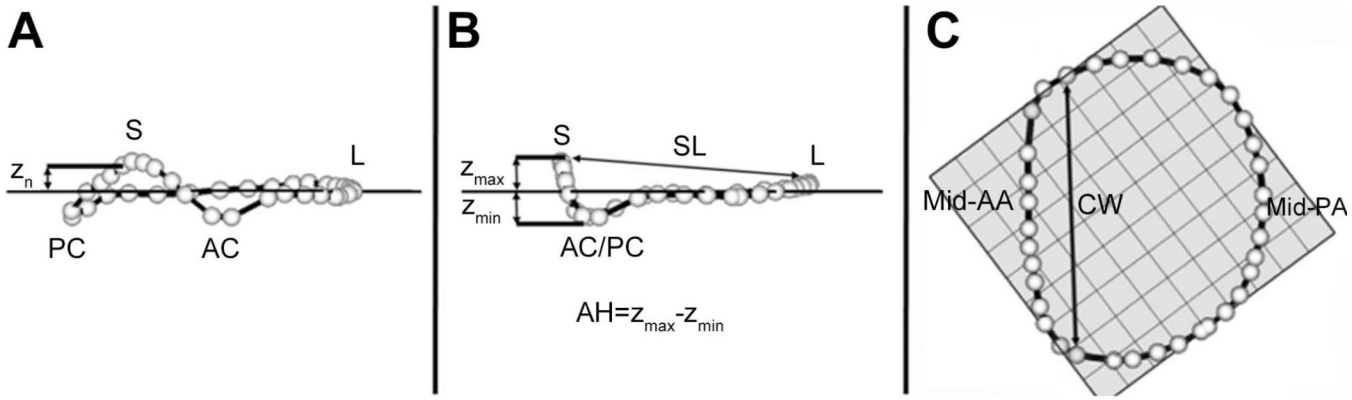

Figure 3. Annular Modeling

Oblique **(A)**, Intercommissural **(B)**, and Transvalvular **(C)** views of a single real-time three-dimensional derived mitral annular model. The 36 annular data points (white spheres) have been included. The least squares plane has been superimposed on the annulus in each view. **Panel A** illustrates the manner in which the distance from the least squares plane to a given annular point (z_n) is measured for a given data point. **Panel B** illustrates the manner in which both annular height (AH) and septolateral diameter (SL) are determined for each valve. **Panel C** illustrates the manner in which the intercommissural width (CW) is determined for each valve. AC: anterior commissure; AH: annular height; AL: antero-lateral point; CW: commissural width; MTD: mitral transverse diameter; PC: posterior commissure; PM: postero-medial point; SL: septolateral diameter; z_n: regional height.

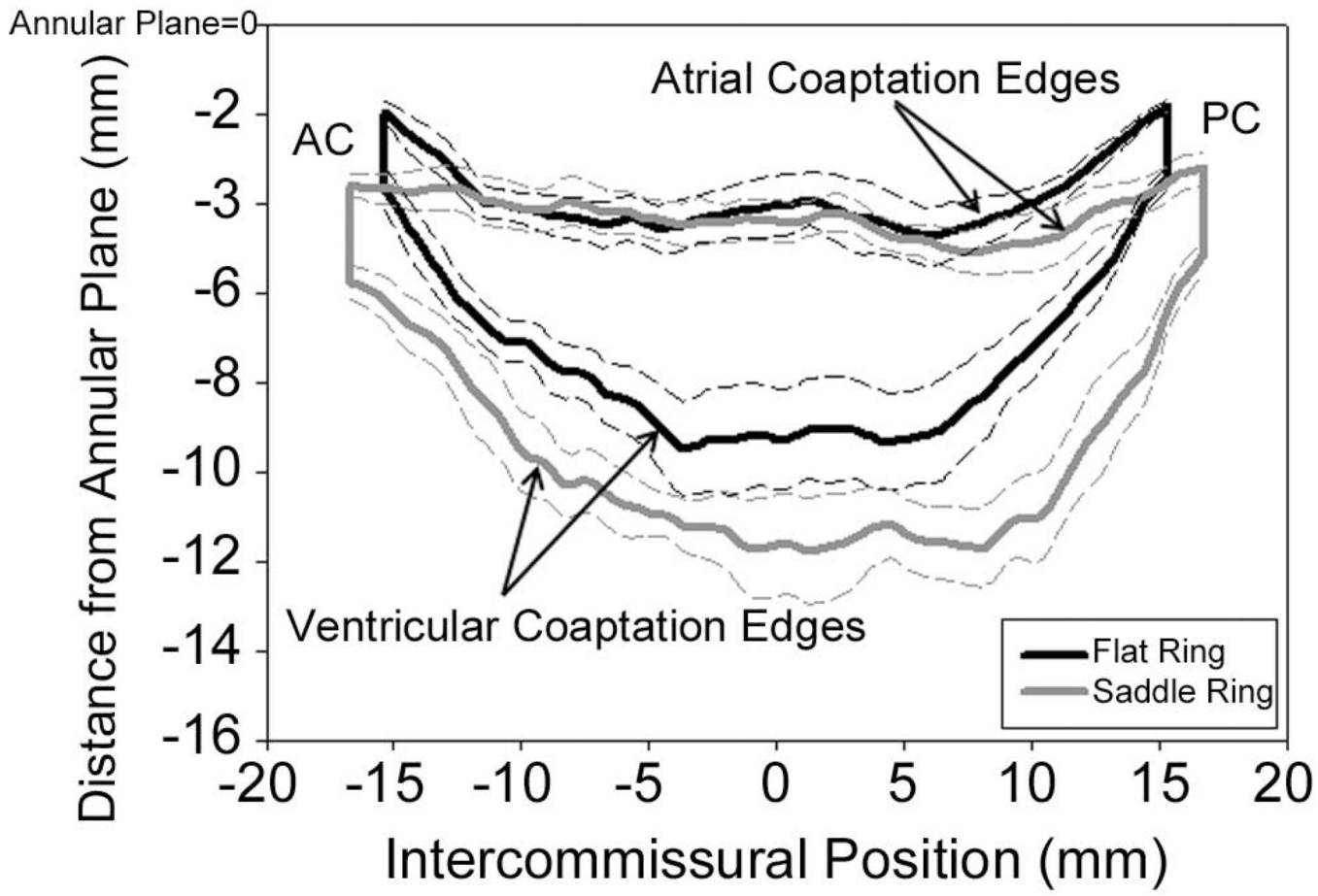

Figure 4. Comparison of Coaptation Area

Black curves represent the 2D projections of the averaged atrial and ventricular coaptation edges for the flat annuloplasty group. The area bounded by the two curves is the projected 2D coaptation area. The grey curves signify similar parameters for the saddle shaped annuloplasty group. The represented viewing plane is orthogonal to the averaged best fit annular plane and passes through the line connecting the anterior (AC) and posterior (PC) commissures. These composite images were created using interpolation of a normalized intercommissural sampling scale for each valve. Dashed lines represent standard deviations. Notice the larger coaptation area of the saddle group and how the flat ring tends to pull the commissures in a more atrial direction.

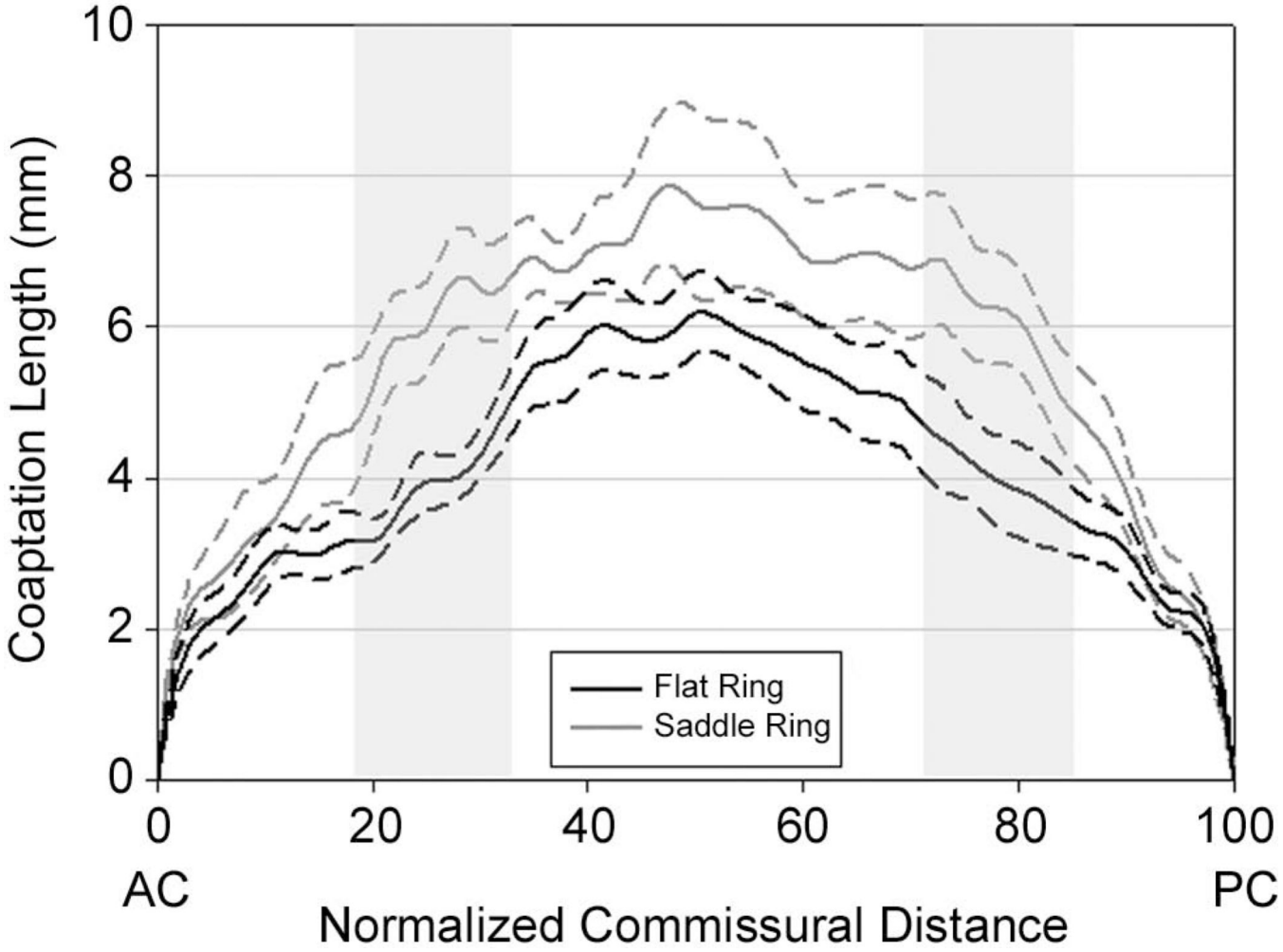

Figure 5. Comparison of Coaptation Length

Graphic presentation of leaflet coaptation length vs. normalized intercommissural position for both the saddle (grey) and flat (black) annuloplasty groups. Dashed lines represent standard deviations. Shaded areas indicate regions were coaptation length differed significantly between groups.

Table 1

Procedure Summary

Saddle Annuloplasty				Flat Annuloplasty			
Flail Segment	**Surgical Technique**	**Ring Size**	**Surgeon**	**Flail Segment**	**Surgical Technique**	**Ring Size**	**Surgeon**
P2	Quadrangular Resection	28	4	P2	Triangular Resection	36	1
P2	Triangular Resection	34	1	P2	Triangular Resection	30	1
P2	Quadrangular Resection	32	3	P3	Triangular Resection	32	2
P2	Quadrangular Resection	38	1	P2	Quadrangular Resection	34	2
P2	Triangular Resection	32	1	P2	Quadrangular Resection	30	2
P2	Quadrangular Resection	30	1	P2	Inversionplasty	32	3
P2	Quadrangular Resection	32	4	P2	Inversionplasty	30	3
P2	Quadrangular Resection	30	4	P2	Triangular Resection	32	2

Table 2

Annular and Leaflet Data Summary

	Flat Ring	Saddle Ring
Pre-Repair Annular Height (mm)	7.2 ± 0.9	7.5 ± 0.6
Post-Repair Annular Height (mm)	2.7 ± 0.2	7.7 ± 0.5*
Pre-Repair Commissural Width (mm)	35.3 ± 2.1	37.0 ± 2.1
Post-Repair Commissural Width (mm)	30.7 ± 0.9	33.5 ± 1.1
Pre-Repair Annular Height Commissural Width Ratio	20.2 ± 1.6	20.5 ± 1.6
Post-Repair Annular Height Commissural Width Ratio	8.7 ± 0.6	22.9 ± 1.2*
Pre-Repair Septolateral Dimension (mm)	33.7 ± 1.6	37.7 ± 1.8
Post-Repair Septolateral Dimension (mm)	23.7 ± 0.5	23.6 ± 0.8
Pre-Repair Mitral Annular Area (mm^2)	1228.5 ± 99.8	1461.9 ± 149.4
Post-Repair Mitral Annular Area (mm^2)	588.6 ± 26.5	628.0 ± 35.3
Annular Undersizing (%)	−50.7 ± 2.8	−54.6 ± 4.2
Post-Repair Total Surface Area (mm^2)	2198.5 ± 151.6	2303.9 ± 183.8
Post-Repair Coaptation (mm^2)	154.0 ± 13.0	226.8 ± 24.0*
Post-Repair Coaptation / Diastolic Surface Area	0.07 ± 0.00	0.10 ± 0.01*
Normalized Coaptation Area (mm^2)	41.2 ± 2.7	62.6 ± 7.7*
3D Atrial Coaptation Edge Length (mm)	28.4 ± 0.8	31.3 ± 1.0*
3D Ventricular Coaptation Edge Length (mm)	28.4 ± 0.8	31.3 ± 1.0*

* denotes significant between group differences ($p<0.05$)